SUPPLEMENTARY FIGURES

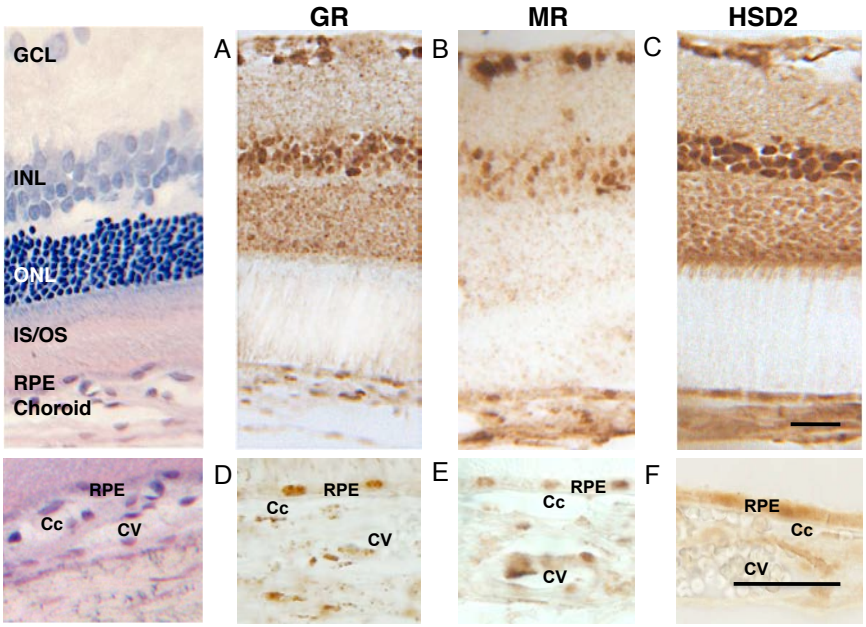

Figure S1

Figure S1: Immunohistochemistry evidence for glucocorticoid receptor (GR), mineralocorticoid receptor (MR) and 11-beta hydroxysteroid dehydrogenase type 2 (HSD2) expression in the rat retina and choroid.
The left panel shows the morphology of the retina with the different cell layers. Lower panels are enlargements of the choroid zone.
GR is expressed in the GCL, INL and ONL of the neuroretina, in the RPE cells and in endothelial cells of choroidal vessels (A and D).
MR is expressed in GCL and INL in the neuroretina, also in RPE cells and in choroidal endothelial cells (B and E).
HSD2 is expressed in GCL, INL and ONL in the neuroretina and also in RPE cells (C and F). HSD2 is faintly expressed in endothelial cells in choroidal vessels (F), precluding efficient glucocorticoid clearance. Abbreviations are provided in Methods section.
Bar = 20µm.

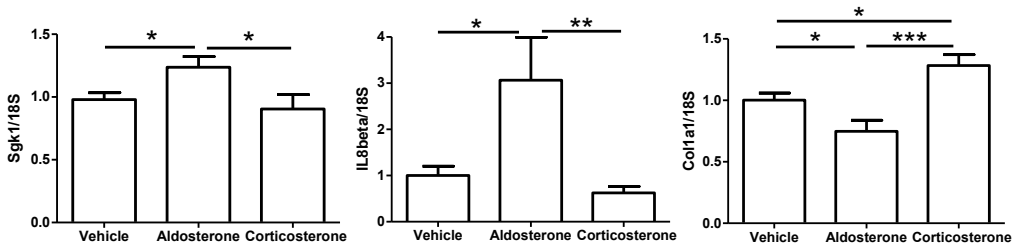

Figure S2

Figure S2: Differential effects of aldosterone and glucocorticoids on gene expression in rat choroid samples.

Rat eyes were injected IVT with NaCl (vehicle), aldosterone (20nM) or corticosterone (1μM) 24 hrs before sacrifice. The RPE-choroid-sclera complex was dissected from the neuroretina and samples were processed for Q-PCR analysis. Reference gene was 18S; results are expressed relative to vehicle-injected eyes. Aldosterone up-regulated the mRNA encoding for serum and glucocorticoid-induced kinase 1 (sgk1) and interleukine 8 beta (Il8 beta) and down-regulated collagen I alpha1 (Col1a1); conversely corticosterone increased the expression of Col1a1, not sgk1 or Il8 beta, indicating that distinct mineralo- and glucocorticoid pathways are functional.

n=5-12 rats per condition. * $P<0.05$, ** $P<0.01$, *** $P<0.001$.

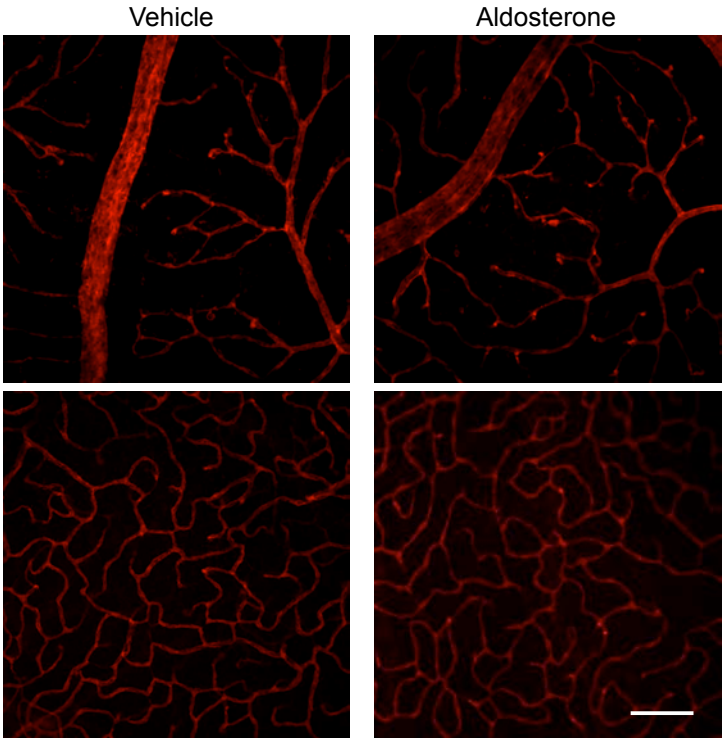

Figure S3

Figure S3: Rat retinal vessels are not dilated following aldosterone treatment.
Rat eyes were injected IVT with NaCl (vehicle) or aldosterone (20nM) and the neuroretina was dissected and flat-mounted. Retinal vessels were labeled with TRITC-labeled lectin from Bandeiraea Simplicifolia. Confocal images show that neither the large retinal vessels (upper photographs) nor the capillary network (lower photographs) of the neuroretina are modified by aldosterone injection.
Bar = 100µm

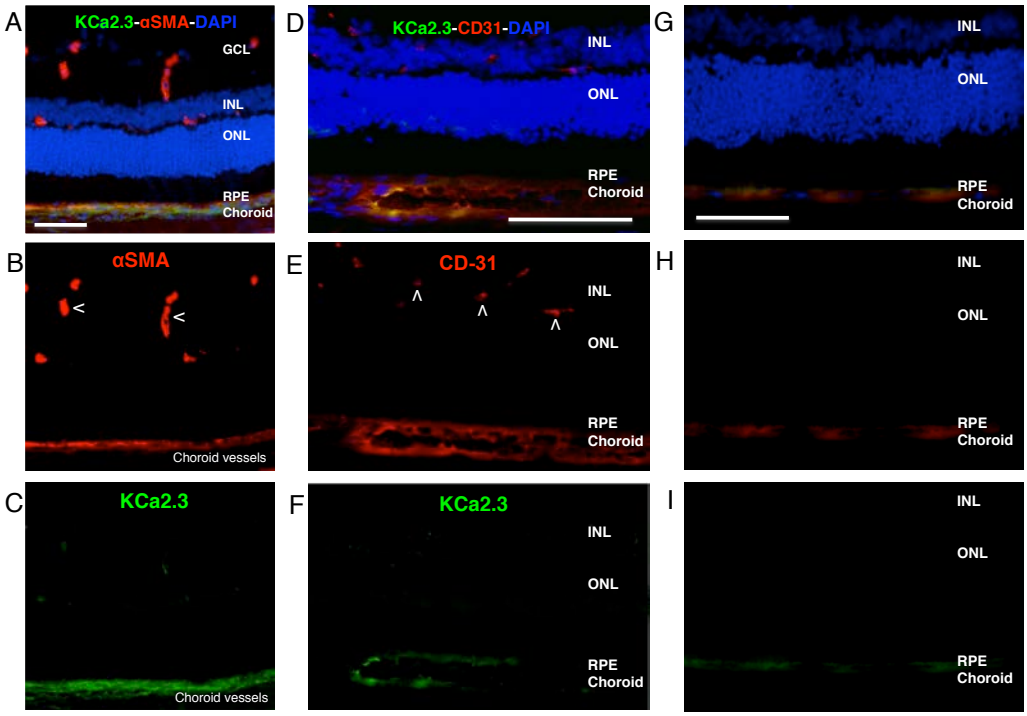

Figure S4

Figure S4: Immunolocalization of KCa2.3 in the rat neuroretina and choroid: KCa2.3 is expressed in the endothelium of choroid vessels.

A-C: photographs of a rat eye section incubated with antibodies against α-SMA (red) and KCa2.3 (green) and the merge image (A). Retinal vessels (arrowheads) that express α-SMA express very faint KCa2.3 signal, whilst choroidal vessels express both α -SMA and KCa2.3.

D-F: photographs of eye section of another rat incubated with antibodies against CD-31 (red) and KCa2.3 (green) and the merge image (D). KCa2.3 signal is colocalized with CD31, a marker of the endothelium (D-F) in choroid, while retinal vessels (arrowheads) labeled with CD31 antibody (panel E) do not exhibit KCa2.3 signal (panel F).

G-I: photographs of another rat eye section incubated without primary antibody, showing background signal.

Nuclei are stained with DAPI (blue). Abbreviations are provided in Methods section.

Bar = 100μm.

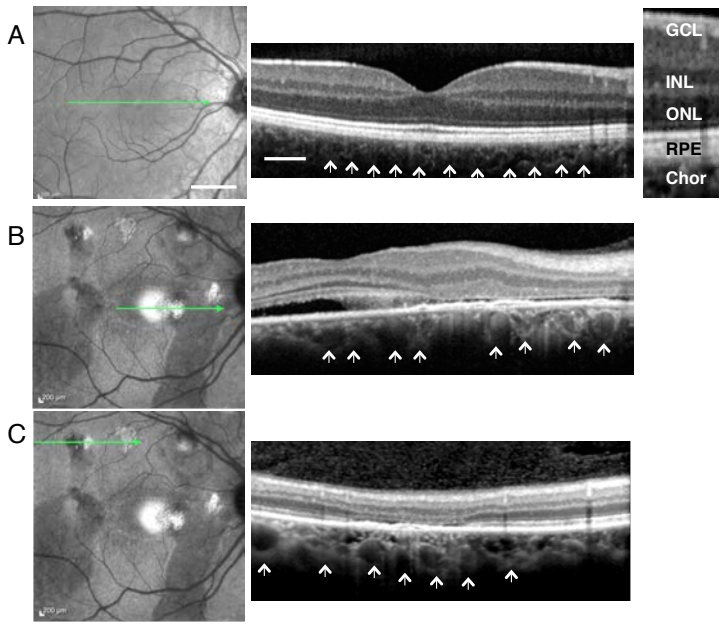

Figure S5

Figure S5: Human eye fundus and Optical Coherence Tomography (OCT) of chronic CSCR in humans shows choroidal vasodilation and retinal detachment.
A: fundus photography (left) and OCT (right) of a normal human eye, showing normal choroid thickness and the different retinal layers.
B and C: fundus photography (left) and OCT (right) of a patient with chronic CSCR.
OCT sections are realized in zones selected on the fundus images (green arrows of the left panels). In these zones, corresponding OCT sections (right panels) show choroidal vessels dilation with increased choroid thickness. The lower limit of the choroid is delineated by the small arrows. Abbreviations are provided in Methods section.
Bar = 2mm for fundus photography and 200μm for OCT.

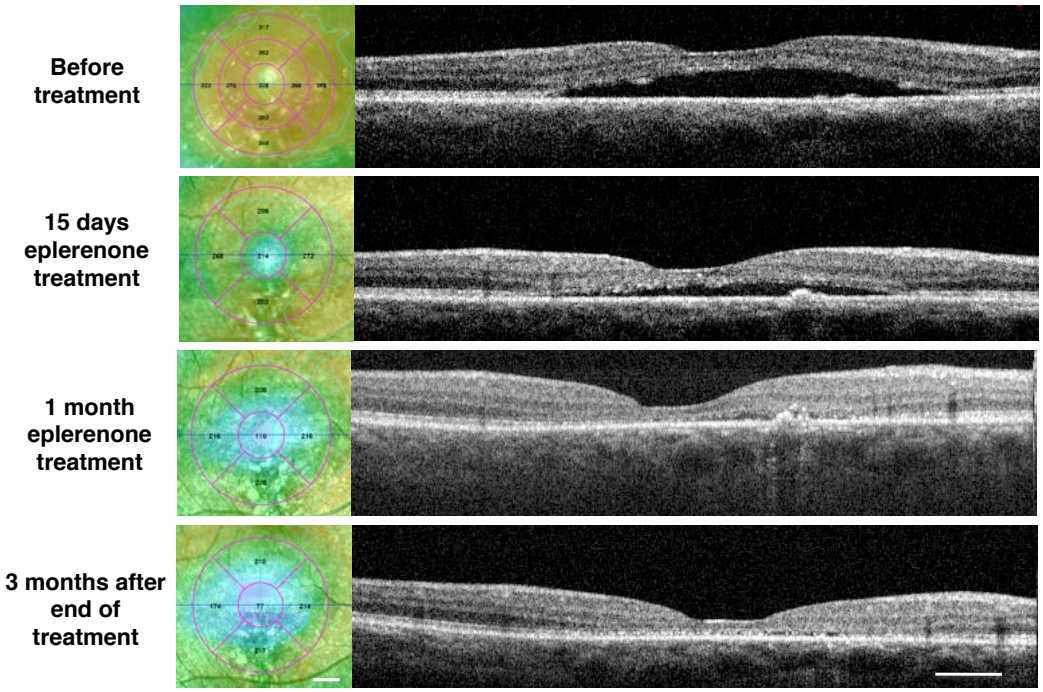

Figure S6

Figure S6: Improvement of retinal serous detachment in patient 3 after eplerenone treatment.

Optical Coherence Tomography (right panels) shows the rapid improvement of serous retinal detachment following onset of eplerenone treatment that remained stable for 3 months after the end of the treatment. Color mapping representation of the retinal surface (left panels) shows red areas illustrating the extent of the retinal detachment. Bar = 2mm for color mapping and 400µm for OCT.

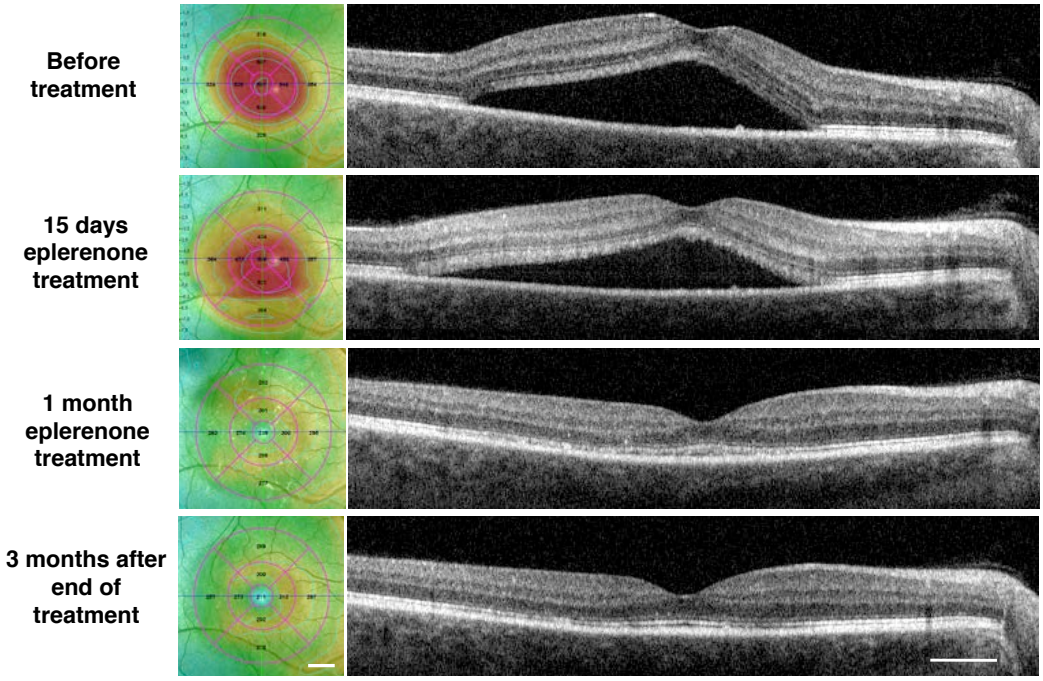

Figure S7

Figure S7: Improvement of retinal serous detachment in patient 4 after eplerenone treatment.

Optical Coherence Tomography (right panels) shows the improvement of serous retinal detachment following onset of eplerenone treatment that remained stable for 3 months after the end of the treatment. Color mapping representation of the retinal surface (left panels) shows red areas illustrating the extent of the retinal detachment. Bar = 2mm for color mapping and 400µm for OCT.

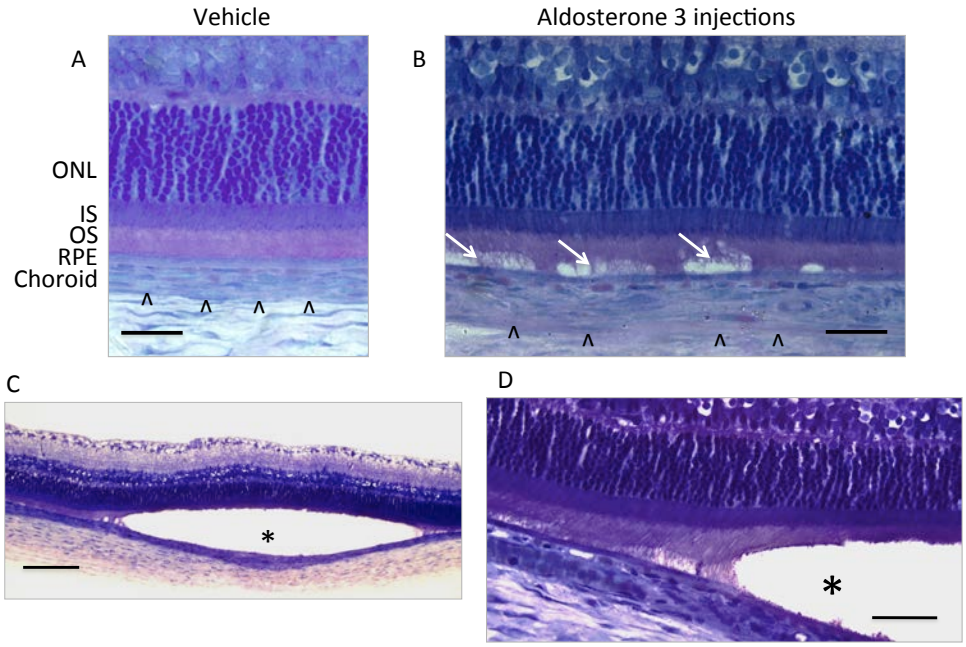

Figure S8

Figure S8: Subretinal detachment induced by 3 iterative injections of aldosterone in rat eye.

Aldosterone (20 nM) was injected IVT on day 0, 2 and 4, and rats were sacrificed on day 6. Historesine sections show variable degree of subretinal detachment after aldosterone treatment (panel B, arrows; panels C and D, star), compared to vehicle-injected eye (panel A). Arrowheads indicate the limit of the choroid. Bar = 50 μm in A and B, 150 μm in C, and 60 μm in D. Abbreviations are provided in Methods section.

SUPPLEMENTARY METHODS

Real time PCR:

RNA isolation, processing and Q-PCR analysis were performed as described (M. Zhao et al, FASEB J 2010, 24:3405-15), using either Taqman (for IL8 beta) or Sybrgreen (for sgk1 and Col1a1) methodology. Primers for Sybrgreen were as follows: sgk1: forward: CCACCTTCTGTGGCACGCCT; reverse: CTCGGCTGTGTTCCGGCTGT; Col1a1: forward: AAACACCCCAGCGAAGAA; reverse: CTGAGTTGCCATTTCCTTGGA; 18S: forward: CGCCGCTAGAGGTGAAATTC; reverse: TCTTGGCAAATGCTTTCGC. Taqman primers (Applied Biosystems patent) were used for IL8 beta and 18S.

Visualisation of retinal vessels:

Rat flat mount retinas were prepared as previously described and retinal vessels were stained with TRITC-labeled lectin from Bandeiraea Simplicifolia (M. Zhao et al, FASEB J 2010, 24:3405-15) images were taken with a confocal laser scanning microscope Zeiss LSM 710.